ADDITIVE REPAIR DESIGN APPROACH: CASE STUDY TO REPAIR ALUMINIUM BASE COMPONENTS

Zghair, Yousif Amsad; Lachmayer, Roland
Leibniz Universität Hannover, Germany

Abstract

Additive manufacturing is considered one of the modest manufacturing techniques. Using this technique in components repair is the state of the art in the industry of maintenance. This paper introduces an additive repair design approach, with focus on Selective Laser Melting technique, and investigates mechanical properties and the bonding force between the damaged components and the added repaired volume. Various load cases and building directions are discussed, and a selected one is simulated and applied on a case study. The candidate metals of the damaged parts are Al-6082 and Al-7075 alloys, and the used powder to repair with the Selective Laser Melting machine is AlSi10Mg. The analysis carried out by means of a finite element numerical model to estimate the axial loading and the induced stresses. Experimental work is implemented, and all analytical and experimental results are discussed and compared. This work aims to develop scientific basics for parts repair using additive manufacturing technologies. Overall, the additive repair approach promises efficiency, but has to be further advanced in the field of maintenance for components in industry.

Keywords: Design for Additive Repair, Design for Additive Manufacturing (DfAM), Additive Manufacturing, Design methods, Computer Aided Design (CAD)

Contact:
Yousif Amsad Zghair
Leibniz Universität Hannover
Institute for Product Development
Germany
zghair@ipeg.uni-hannover.de

Please cite this paper as:
Surnames, Initials: *Title of paper*. In: Proceedings of the 21st International Conference on Engineering Design (ICED17), Vol. 5: Design for X, Design to X, Vancouver, Canada, 21.-25.08.2017.

1 INTRODUCTION

Due to the continues improvements of Additive Manufacturing technologies (AM) such as high building speeds, enhanced reliability and quality or increased precision, a progressive establishment in a great variety of applications can be noticed. In addition to additively manufactured tools, AM parts are partially integrated in assemblies and thus used professional practice (Lachmayer and others, 2016). Components usually suffer from wear, distortion, defects and cracks during their life cycle, and sometimes repairing is considered most cost effective and time saving than replacing these components. For a complex geometry, especially aerospace components, the repair process gets more complicated, and the traditional repair methods cannot be used for. Therefore, introducing new solutions by using additive manufacturing techniques to repair parts is a necessity in the industrial world (Zghair, 2016). Since the additive technologies are used in repair, Zghair (2016) has defined the term "Additive Repair (AR)" as "*additive manufacturing process for reconstruct and modify prebuilt components*". So, it is an additive manufacturing process, but to build over pre-existing components manufactured from the same base metal or different metals. Additive manufacturing technology can be found in applications like laser repair and laser freeform manufacturing. Companies like RPM Innovations, have already provided services using laser deposition technologies, such as laser engineered net shaping, advanced additive manufacturing and repair and laser repair technology (LRT). Huan and Magdi (2010) used Laser powder deposition based method called Laser Net Shape Manufacturing LNSM to repair turbine compressor airfoil in his research due to the advantage of fine microstructure, small heat affected zone and superior to cast material properties, and they develop a geometry-based adaptive toolpath deposition method for the repair of compressor or blisk airfoils with Inconel 718 alloy. The Collaborative Research Centre (CRC) 871 "Regeneration of Complex Capital Goods" developed a laser cladding process for crack repair, this process can create a single-crystalline solidification of the cladding material. This method is used to repair the turbines blades, therefore nickel base-alloys are used (Nicolaus and others, 2015). Siemens Company has already used additive repair technology to repair gas turbines, it used Selective Laser Melting (SLM) technology to repair gas turbines burner's tips. The process is to add metal powder layer by layer equally over a pre-machined plane surface, which represent a reference plane to start build the damaged volume of the burner. The company used a modified SLM machine that used for additive manufacturing. Data and facts clearly detail the success of the new repair process. Siemens will be able to reduce repair time by 90% compared to conventional repair procedures, a significant improvement. This is also an opportunity to modify repaired components to the latest burner design (Navrotsky and others, 2015). EOS Company for additive manufacturing solutions stated on its web site the possibility to use additive manufacturing in order to repair damaged tool inserts, it used also SLM technology to perform these repairs, saving manufacturers time and money. "The experimental results show also that the parts built-up additively by SLM (part of an aluminium extrusion die) withstand the high mechanical and thermal loads which occur during hot aluminium extrusion", and also "the hybrid components are on a comparable level of strength as the conventionally manufactured" Hölker and Tekkaya (2016) said. Among diverse established additive layer manufacturing technologies, SLM has become a promising manufacturing route for engineering parts. It is a rapid manufacturing technique which enables prompt modelling of metal objects with defined structure and shape of complex geometry on the basis of virtual 3D model data. It considered one of the best manufacturing techniques in laser sintering due to its great potentiality in direct production (Capello and others, 2005). Contributing SLM technology within machine element repair is a big challenge, because of all variants surrounding the element in its working space, or the process limitations. Due to the wide range of applications in aircraft and automotive industry, this paper will focus on aluminium components. A general additive repair design process is defined, and will be investigated to facilitate the steps required to perform an additive repair for components. Since SLM can only build on flat planes, four possible building procedures of the added volume are introduced to satisfy the load type and magnitude. Later three load cases are defined, and the possible solutions to design the added volume are discussed. One of these load cases is selected, and one of the possible solutions is implemented theoretically and practically for two selected aluminium alloys by taking a tensile test specimen as a demonstrator. Finally, the results are compared and discussed.

2 ADDITIVE REPAIR DESIGN PROCESS APPROACH

It is the designer's responsibility to ensure that a machine part is safe for operation under reasonably expected conditions. All design approaches must verify the relationship between the applied stresses on a part and the strength of its metal (Ponche and others, 2012). By taking all the advantages of the additive manufacturing process, and specifying all of its capabilities and constraints, the designing process can be modified by AM technologies (Vayre and others, 2012). The objective of this computer based design process approach is to define a methodology to design the damaged volume of parts by taking the advantage of additive manufacturing abilities. In the early design phase, the engineer has to make a design concept for the missing volume of the damaged part. Hence, he need some solutions principals, methods and tools to help in embodiment the design. Therefore, this methodology will help to set a design principals that the designer can follow to make first conceptual draft. This methodology consists of two main steps (Figure 1). The first one is to define a new metals library, in which each metal alloy powder is assigned to be weldable with several metal alloys. By doing so, it would be possible to know which powder fits to the metal of the part intended to repair, and the bonding between the two metals is strong enough to carry the same designed loads. After the specifications of the part to be repaired are proposed, the added repaired volume can be designed. The designer has to consider the stress concentration zones, the position of interface surface (where the added volume will start from), the building direction and number of building stages. For the interface plane position, it is important for designers to avoid the stress concentration planes in the remaining volume of the part to be repaired. Therefore, designer can select the interface surface location away from the fracture zone to avoid high stresses and cracks propagations. According to the load magnitude and way of application, and geometry complicity, the interface surface profile and number of building stages are determined. The designer has also the possibility to modify the added repaired volume in accordance with service conditions, and optimizing in relation to the specifications and the manufacturing constraints and design space. This process approach needs to be verified step by step to set up the solution principals. The later work in this paper is a start to create simple metal library, and to verify the process stages for one simple load case, and to be extended in future for other metals and load cases.

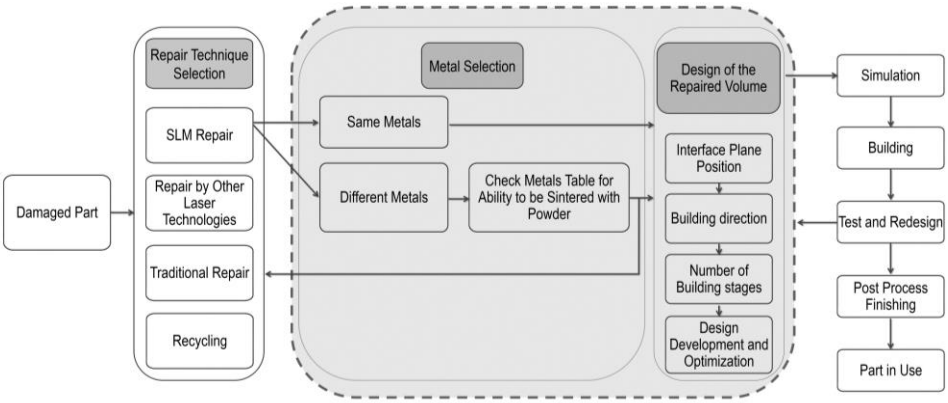

Figure 1. Concept of design process approach for additive repair.

2.1 Possible building-over directions

SLM machines can only build on flat plane surfaces in the upward direction. Therefore, it is necessary to prepare the damaged part prior to the building process. The preparation is done by cutting the damaged part from a certain position and a certain angle to get plane surface. The position and angle of the cut eventually define the form of the oblique plane. It is possible to define more than one oblique plane for the same cut position. The load type and magnitude play a big role in identifying the suitable cut position and angle. Figure 2 shows that the building process could be divided into three stages, and each stage represents a separate complete process. This means that each stage will be prepared separately from the other stages, and it will have its own parameters and requirements, such as laser parameters, atmosphere gas used, part mounting facilities, etc. The selection of the suitable building method depends on the design and shape of the fractured area and the type of loads that the part has to endure during operation.

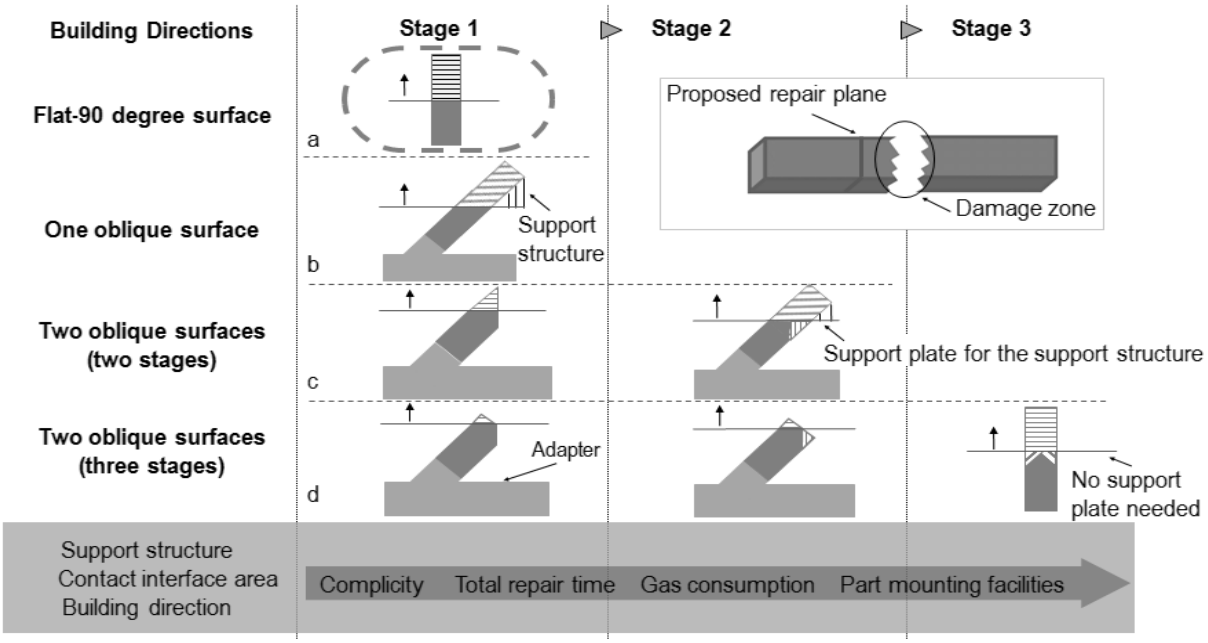

Figure 2. Building directions and planes. a) Flat surface, one building stage. b) One oblique surface, one building stage. c) Two oblique surfaces, two building stages. d) Two oblique surfaces, two building stages.

2.2 Load cases and interface surface building angle

All mechanical parts are subjected to variants of static or dynamic loads during operation. The loads are mainly tension, compression, torsion or bending loads, and in many cases it is a combination of more than one of them. The building direction in SLM is crucial, and the metal produced is orthotropic (Zghair and others, 2016; Strößner and others, 2015). The manner of computing the design stress depends on the manner of loading and on the type of material being used. The load could be static, repeated and reversed, fluctuating, shock or impact and random. Three types of loading cases are proposed in this work, and three solutions for each load case are suggested (Figure 3). These solutions depend on the possible building directions with SLM machines. But the selection of the optional design of the damaged zone depends on the type of subjected load and stress concentration points. All parts are considered to be subjected to static loads that are applied slowly, without shock, and are held at constant values. Hence all resulting stresses are static. In this case the maximum and minimum stresses are the same. Since the maximum shear stress in tension loads leis in the 45° plan, therefore the one and two oblique interface profiles will not be implemented to avoid subjecting the interface surface to this maximum shear stress. In this paper, the first case of tension load subjected on component with flat interface surface profile will be investigated, and the induced stresses will be analysed numerically, and will be compared with the experimental results.

There are some assumptions to be made to design the fracture zone of the damaged part when it is subjected to axial load. The load is assumed to be static, hence the resulting stress is static. The longitudinal dimension of the part is greater than the other dimensions. The force is coinciding with the longitudinal axis of the part so that there is only uniaxial loading, and no bending of the part. After subjecting the part to axial loading, resisting forces are set up within the interface plane between the damaged part and the added sintered volume.

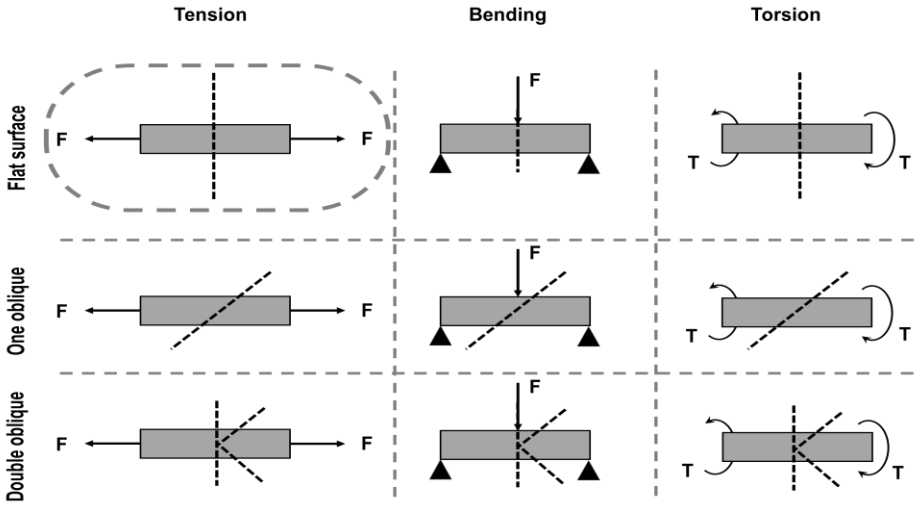

Figure 3. Load cases and the interface surface building angles.

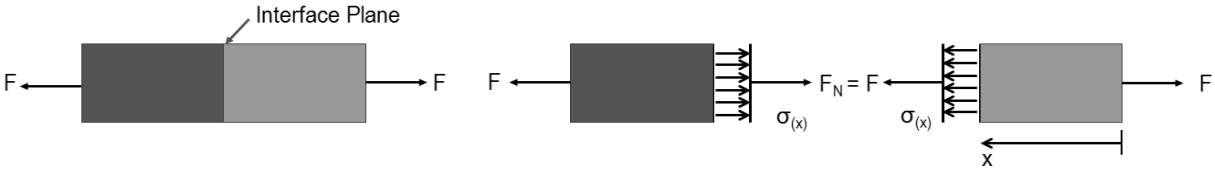

Figure 4. Stress induced in longitudinal loading case in a 90∘plane.

The free body diagram (Figure 4) shows the resisting forces produced in the interface plane. For equilibrium condition, the horizontal resisting distributed forces are equal to the external applied force F, and assumed to be distributed uniformly across the interface plane. The resulting stress of this acting force on the interface surface is a normal stress, and can be expressed in Equation (1) as:

$$\sigma_N = \sigma_{(x)} = \frac{F}{A} \tag{1}$$

Where σ_N is the normal stress, $\sigma_{(x)}$ is the stress at distance x and A is the area of the interface plane.

3 CASE STUDY OF STATIC TENSION LOAD

3.1 Materials used

Commercial heat treatable Al alloys are 2000 (Al-Cu or Al-Cu-Mg), 6000 (Al-Si-Mg), and 7000 (Al-Zn-Mg) series alloys, whose properties are enhanced by various heat treatment processes. Among the 6000 alloys, the 6082 with high content of magnesium and silicon is selected. It is the strongest alloy with widespread applications in building, aircraft and automotive industry (Kempen and others, 2012). An aluminium alloy of the 7000 series is also selected. The 7075 alloy provides a combination of high strength and high thermal conductivity. It can find its applications in aircraft fittings, gears, shafts and other highly stressed structural parts. Current state-of-the-art of the SLM process focusses on Al-Si powders. These metal powders are relatively easy to process due to the small difference between liquid and solidus temperature compared to high strength aluminium alloys (Bartkowiak and others, 2011). AlSi10Mg is a fine aluminium alloy powder optimized for processing on EOSINT M systems. These material characteristics will be used in the analysis, and this metal will be the repairing metal. Table 1 shows the properties of the three selected aluminium alloys.

Table 1. Mechanical properties of selected aluminium alloys

	Ultimate strength [MPa.]	Offset 0.2% (Rp0.2) [MPa.]	Total deformation [%]	Elastic module [MPa.]
AlSi10Mg	345	220	7	65.000
Al-6082	280	200	12	70.000
Al-7075	490	400	6	72.000

3.2 Digital specimens model

To predict the stresses induced in the interface surface of a repaired part in tension load, and to evaluate the bonding strength of this surface, a tensile test specimen is investigated as the case study model. The known stress distribution and the expected position of the fracture point are reasons to choose the specimen as the case study model. In tensile tests of homogenous metals, the candidate area for fracture is located in the gauge length of the specimen, and it will be close to the middle. Therefore the interface surface is positioned in the middle of the specimen, to simulate a real fracture case, and to subject the surface to highest stress. The dimensions of the specimen are specified to German standard DIN 50125, and the specimen will be divided into two halves. One half is made of a precast metal, and represents the damaged part, the other half is the sintered metal, and represents the repaired volume (Figure 5).

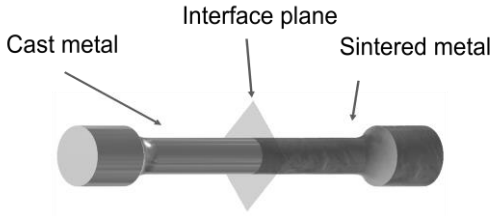

Figure 5. Two metals tensile test specimen model.

3.3 Specimens manufacturing

The building process in AR must be designed for each building job separately. AR has almost the same as SLM process steps, but with extra preparations. The process starts with the design of the volume that will be substituted in the repaired part. This volume has the same or an enhanced geometry and functions. The interface plane design is also included in this step either the laser power required to perform this plane, or the building directions and stages required. Ten specimens are manufactured, and the first half is machined on a lath machine. The raw metals used to manufacture these specimens are Al 6082 and 7075, five specimens of each metal respectively. The other halves are sintered on the top of the machined halves, and the metal powder used is AlSi10Mg. Laser parameters, such as scan rate, layer thickness, distance between paths and laser power are important to build dense parts with proved mechanical properties, and they are related to each other. Increasing the density of the apart will enhance the mechanical properties, and by optimizing one of the four laser parameters one can achieve the optimal energy input for obtaining the highest density for the parts (Kempen and others, 2011). Different laser parameters were used to get the optimal bonding between the two metals. The laser parameters required to sinter the metal powder is set up for each specimen separately, so that there are 10 sets of parameters for the 10 specimens. Each set consists of three different layers parameters, which perform the interface zone. The laser power can be determined by defining a specific laser energy input per unit volume ψ (Olakanmi, 2013; Williams and others, 2015):

$$\psi = \frac{P}{uhd} \tag{2}$$

where P is the laser power (W), u is the scan rate (mm/s), h is the scan spacing (mm) and d is the layer thickness (mm). The layer thickness is configured to 0.3 mm, and the scan spacing to 0.19 mm. Using Equation (2), the laser intensity is adjusted by varying the laser power and mirror speed (see Table 2) (Olakanmi and others, 2015; Murali and others, 2003; Simchi and others, 2004). Then the specimens are machined to the exact dimensions, and annealed for two hours at 300 °C to relieve the residual stress (Figure 6).

Table 2. Range of laser intensity used to form the interface layer for 10 specimens.

Specimen No.	1	2	3	4	5	6	7	8	9	10
Metals	AlSi10Mg with Al-6082					AlSi10Mg with Al-7075				
First layer laser intensity	40.5	45	50	60	70	37.8	43	50	55.5	65.5
Second layer laser intensity	45	47.5	50	55	60	43.8	45.8	50	53	57.7
Third layer laser intensity	50	50	50	50	50	50	50	50	50	50

Figure 6. Specimens building process. a) Half specimens (cast metal) are screwed to adapter with threaded holes. b) Specimens after building c) Specimens after machining to final dimensions.

3.4 Computer aided simulation

In this part of the work, a finite element method is implemented to analyse stresses, deflections in specimens and the location of expected fracture zone. Since the model is made out of two metals and each metal has a different modulus of elasticity, the expected deformations and stresses of each half will not be the same (Figure 7). The tangent modulus of the nonlinear behaviour of the metals is defined in the ANSYS engineering data as bilinear metals (Mišović, Tadić and Lučić, 2016; Yu, Wan, Wu, and Zhou, 2012). After analysis is complete, one observes that the area reduction started in the middle of the weakest metal half, and Von Mises equivalent stress exceeds the uniaxial material yield strength, which means that general yielding will occur in that area first, and consecutively the ultimate stress. For the first model (AlSi10Mg with Al-6082) it is observed that Al-6082 yields first. The maximum deflection at the ultimate stress is 3.86 % (Figure 8). For the second model (AlSi10Mg with Al-7075) the opposite happens. AlSi10Mg yields first, and the maximum deflection at the ultimate stress is 3.8 % (Figure 9).

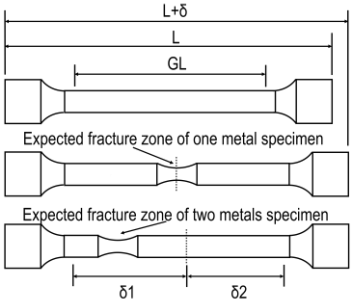

Figure 7. Expected Fracture zone for the specimens manufactured from one and two metals (L is the specimen length, GL is gauge length, δ is the deflection).

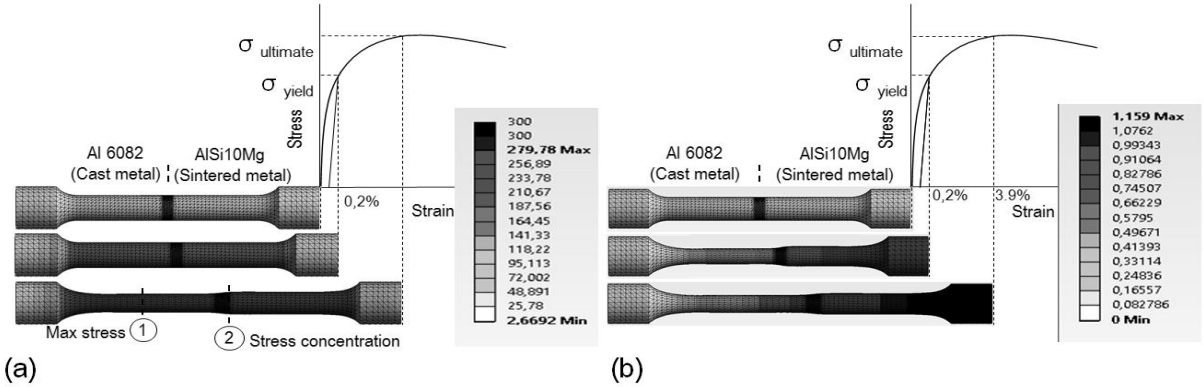

Figure 8. Finite elements analysis of the Al-6082 specimen model. a) Stress analysis. b) Total deformation.

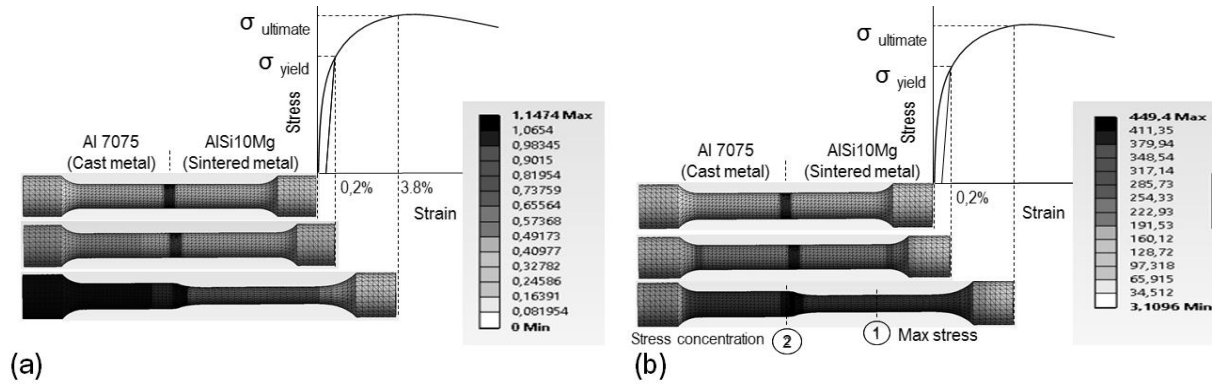

Figure 9. Finite elements analysis of the Al-7075 specimen model. a) Stress analysis. b) Total deformation

3.5 Tensile test analysis

The tensile test for all specimens is conducted at room temperature, and in accordance with DIN EN 6892-1 B. The test results show that four specimens fractured outside the gauge length (Figure 10 a), but this will not be considered because this test does not represent a standard DIN test. Therefore, all fractures that occur outside the gauge length and within the same diameter dimension will be considered. For the first group of specimens that are made of Al-6082 with AlSi10Mg, the ultimate stress exceeds 280 MPa. The average ultimate strain is 3%, and the total elongation is over 10%. No visible cracks or any signs of fracture in the interface zone are observed (Figure 10 b). Fractures occur in the cast part of the specimens of the cast basic structure of Al-6082. All five specimens show improved bonding between the two halves, and they are all considered a positive results for the test. The average ultimate stress and strain of the second group of specimens that are made of Al 7075 with AlSi10Mg is around 260 MPa and 3.1% respectively, while the average total elongation is about 3.6%. Specimen number 9 failed in the middle of the interface surface, while the other specimens are fractured elsewhere. The fracture of the four specimens occurs in the sintered halves, and no visible cracks can be seen in the middle of them. The bounding force in the interface zone of the four specimens was strong enough to stand against the applied force.

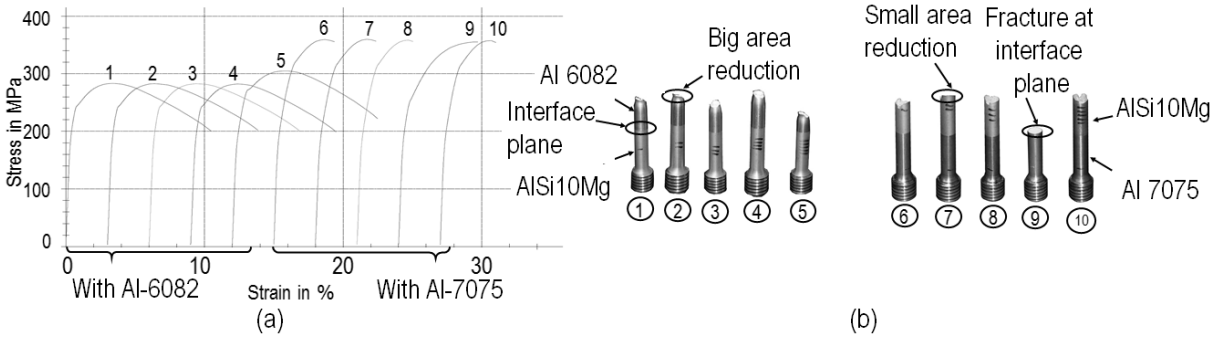

Figure 10. a) Stress-strain curves for the 10 specimen. b) Fractured specimens after tensile test. (1-5) Al-6082 with AlSi10Mg specimens group, (6-10) Al-7075 with AlSi10Mg specimens group.

3.6 Microscopic examination

Microscopic examination regarding the interface between the cast based Al alloy part and the added sintered part was performed. This examination is carried out after the tensile test, and it shows the interface zone under maximum stresses that it can carry out before fracture occurs in the specimens. The samples are etched with sulfuric acid mixture. It can be observed that the laser melts both the powder and the previously cast material (Figure 11), thus forming the interface layer. The laser melts the cast metal to a sufficient depth resulting in an observable homogenous mixture of both metals. The geometry of each single melting pool has a crescent shape, and the difference in colours between the sintered and cast metal is due to the different chemical compositions of the aluminium alloys. No separation at the

interface zone is present, but fails were discovered on all specimens at the interface layer. They are pores, possibly oxide lines or cracks. In the etched state, it is easy to see that the grain is coarse in the interface zone. Since the tensile specimens are not fractured at these points, this does not seem to be a weak point.

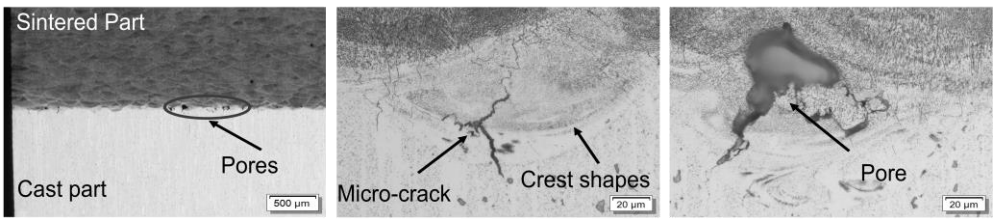

Figure 11. Microscopic pictures for the interface plane between the cast (lower metal) and added sintered metals (upper metal) after tensile test. The samples are etched with sulfuric acid mixture.

4 CONCLUSIONS

Tensile testing on specimens provides uniaxial data, which can easily be plotted on one-dimensional stress-strain curves. The conducted tensile test shows two different curve shapes. The first one is for the Al-8082 cast base alloy, the curve shape is more close to Al-6082 alloy than AlSi10Mg. This is because Al 6082 is softer than the sintered powder, and it yields first. The second curve shape is more close to the sintered powder than the Al-7075, because the sintered powder is softer than the last one. The stress-strain curve obtained from the tensile test is the engineering curve. By locating the maximum stress point in the specimen half which is made of the softer metal, one can draw the stress tensor of that point versus the corresponding strain, taking the area reduction in consideration, and without it. Comparing these three curves for both Al-6082 and Al-7075 with sintered AlSi10Mg respectively, one can calculate the percentage error in the expected strains at the ultimate limit. For AlSi10Mg with Al-6082 deformation error percentage is 28 %, and for AlSi10Mg with Al-7075 deformation error percentage is 18.75% (Figure 12).

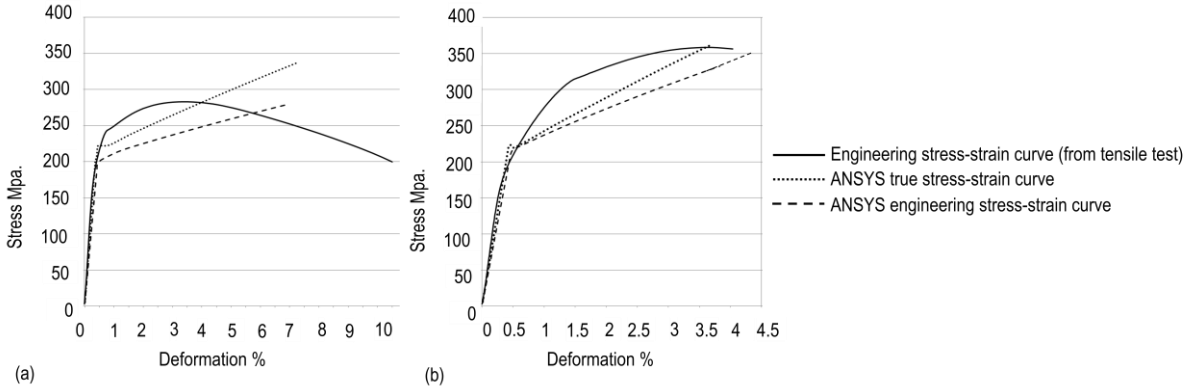

Figure 12. Comparison between true and simulated stress strain curves and the resulting ultimate strain. a) For Al 6082 with AlSi10Mg. b) For Al 7075 with AlSi10Mg.

The bonding between the two metals in the interface zone is strong enough that it can carry the designed loads, and the failure occurs outside it. ANSYS results show accurate results, and predict the failure position exactly. The flat interface surface profile is considered a good choice in the static axial loading. The safety factor for the working stress has to be calculated carefully, because for the case when the sintered metal used in repair is weaker than the original part, then fracture will occur in the repaired volume. To avoid this, the working stress for the repaired part, including the safety factor, must be designed below the yield strength of the sintered metal, or the repaired volume original design must be modified, if possible, to be able to carry the load safely. The laser parameters required to fuse the two metals with powder, the building direction, interface profile and number of building stages are all verified for the given tension load case. Therefore, it possible now to assign these solutions principals to this design process approach for the tension load only, which are: the position of the interface surface

has less effect on its strength, flat interface surface profile is most suitable, and building in the z direction in one stage is possible and will not affect the bonding of the interface surface. Further work will be implemented to enrich the metals library and to verify the other static and dynamic load cases to increase the solution space within this process.

REFERENCES

Bartkowiak, K., Ullrich, S., Frick, T., Schmidt, M, (2011), "New Developments of Laser Processing Aluminium Alloys via Additive Manufacturing Technique", *Physics Procedia*, Volume 12, Part A, pp. 393-401.

Capello, E., Colombo, D., Previtali, B. (2005), "Repairing of sintered tools using laser cladding by wire", Journal *of Materials Processing Technology*, Vol. 164–165, pp. 990–1000.

Hölker, R., Tekkaya, A.E. (2016), "Advancements in the manufacturing of dies for hot aluminium extrusion with conformal cooling channels", *The International Journal of Advanced Manufacturing Technology*, Vol. 83, No. 5, pp. 1209–1220.

Huan, Q., Magdi, A., Singh, Prabhjot (2009), "Adaptive tool path deposition method for laser net shape manufacturing and repair of turbine compressor airfoils" *The International Journal of Advanced Manufacturing Technology*, Vol. 48, No. 1, pp. 121–131.

Kempen, K., Thijs, L., Yasa, E., Badrossamay, M., Verheecke, W., Kruth, J.-P. (2011), "Process Optimization and Microstructural Analysis for Selective Laser Melting of AlSi10Mg", *Solid Freeform Fabrication Symposium (SFF2011)*, Austin (Texas), pp. 484-495.

Kempen, K., Thijs, L., Humbeeck, J., Kruth, J.-P. (2012) "Mechanical properties of AlSi10Mg produced by Selective Laser Melting", *Physics Procedia*, Vol. 39, pp. 439–446.

Lachmayer, R., Lippert, R.B, Fahlbusch, T. (Hrsg.), *3D-Druck beleuchtet – Additive Manufacturing auf dem Weg in die Anwendung*, Springer Vieweg Verlag, Berlin Heidelberg, pp. 57-69. ISBN: 978-3-662-49055-6.

Mišović, M., Tadić, N., Lučić, D. (2016), "Deformation characteristics of aluminium alloys", *GRAĐEVINAR* Vol. 68, No. 3, pp. 179-189.

Murali, K., Chatterjee, A.N., Saha, P., Palai, R., Kumar, S., Roy, S.K., Mishra, P.K., Roy Choudhury, A. (2003), "Direct selective laser sintering of iron–graphite powder mixture", *Journal of Materials Processing Technology*, Vol. 136, No. 1-3, pp. 179–185.

Navrotsky, V., Graichen, A., Brodin, H. (2015), Industrialisation of 3D printing (additive manufacturing) for gas turbine components repair and manufacturing. *VGB Power Tech – Autorenexemplar*. Available at: (http://www.energy.siemens.com/hq/pool/hq/services/industrial-applications/additive-manufacturing/VGB-PowerTech-2015-12-NAVROTSKY-Autorenexemplar.pdf).

Nicolaus, M., Rottwinkel, B., Möhwald, K., Nölke, C., Kaierle, S., Maier, H., Wesling, V. (2015), *Future Regeneration Processes for High Pressure Turbine Blade, Deutscher Luft- und Raumfahrtkongress. Available at: (http://www.dglr.de/publikationen/2015/370119.pdf).*

Olakanmi, E.O. (2013), "Selective laser sintering/melting (SLS/SLM) of pure Al, Al–Mg, and Al–Si powders: Effect of processing conditions and powder properties", *Journal of Materials Processing Technology*, Vol. 213, No.8, pp. 1387–1405.

Olakanmi, E. O., Cochranea, R. F., Dalgarnoc, K. W. (2015), "A review on selective laser sintering/melting (SLS/SLM) of aluminium alloy powders: Processing, microstructure, and properties" *Progress in Materials Science*, Vol. 74, pp 401–477.

Ponche, R., Hascoet, J.Y., Kerbrat, O., Mognol, P. (2012), "A new global approach to design for additive manufacturing", *journal of Virtual and Physical Prototyping*, Vol. 7, No. 2, pp. 93-105.

Simchi, A., Pohl, H. (2004), "Direct laser sintering of iron–graphite powder mixture", *Materials Science and Engineering*, Vol. 383, No. 2, pp. 191–200.

Strößner, J., Terock, M., Glatzel, U. (2015), "Mechanical and Microstructural Investigation of Nickel-Based Superalloy IN718 Manufactured by Selective Laser Melting (SLM)", *Advanced Engineering Materials*, Vol. 17, No. 8, pp. 1099–1105, DOI 10.1002/adem.201500158.

Vayre, B., Vignat, F., Villeneuve, F. (2012), "Designing for Additive Manufacturing", *45th CIRP Conference on Manufacturing Systems*, Vol. 3, pp. 632-637.

Williams, S., Zhao, H., Leonard, F., Derguti, F., Todd, I., Prangnell, P.B. (2015), "XCT Analysis of the Influence of Melt strategies on Defect Population in Ti-6Al-4V Components Manufactured by Selective Electron Beam Melting", *Journal of Materials Characterization*, Vol. 102, pp. 47-61.

Yu, Y., Wan, M., Wu, X., Zhou, X. (2002), "Design of a Cruciform Biaxial Tensile Specimen for Limit Strain Analysis by FEM.", *Journal of Materials Processing Technology*, Vol. 123, No. 1, pp. 67-70.

Zghair, Y. 2016., " Rapid Repair hochwertiger Investitionsgüter ", In: Lachmayer, R., Lippert, R.B., Fahlbusch, T. (Hrsg.), *3D-Druck beleuchtet – Additive Manufacturing auf dem Weg in die Anwendung*, Springer Vieweg Verlag, Berlin Heidelberg, pp. 57-69. ISBN: 978-3-662-49055-6.

Zghair, Y., A., Lachmayer, R., Klose, C., Nürnberger, R. (2016), "Introducing Selective Laser Melting to Manufacture Machine Elements", *International Design Conference - Design 2016*, Cavtat, Dubrovnik, Croatia, May, 16-19, pp. 831-842.